

**Bogdan Wendler¹, Tomasz Moskalewicz², Dariusz Rudnik³, Sławomir Zimowski⁴, Marcin Kot⁴
Marcin Grobelny³, Wojciech Pawlak¹, Adam Rylski¹, Aleksandra Czyrska-Filemonowicz²
Marcin Makówka¹, Piotr Nolbrzak¹, Katarzyna Włodarczyk¹**

¹ Lodz University of Technology, Institute of Materials Science and Engineering, ul. Stefanowskiego 1, 90-924 Lodz, Poland

² AGH University of Science and Technology, Faculty of Metals Engineering and Industrial Computer Science

International Centre of Electron Microscopy for Materials Science, al. Mickiewicza 30, 30-059 Krakow, Poland

³ Motor Transport Institute, ul. Jagiellońska 80, 03-301 Warsaw, Poland

⁴ AGH University of Science and Technology, Faculty of Mechanical Engineering and Robotics, Science, al. Mickiewicza 30, 30-059 Kraków, Poland

Corresponding author: E-mail: bogdan.wendler@p.lodz.pl

Received (Otrzymano) 19.01.2013

NANOCOMPOSITE CARBON- OR MoS₂-BASED SELFLUBRICATING COATINGS FOR AUTOMOTIVE, AVIATION AND SPACECRAFT INDUSTRIES

Higher performance and reliability, reduced fuel and lubricant consumption as well as a greater solicitude to the earth's environment are nowadays the main driving forces of progress in contemporary automotive, aviation and spacecraft industries. Among the effective solutions of these issues are friction reduction in the powertrains of vehicles as well as mass reduction of engines by means of the replacement of steel parts of engines or other mechanisms by twice lighter ones made from titanium alloys. In the paper, basic information concerning the manufacturing of two types of thick carbon or MoS₂-based friction reducing nanocomposite coatings is given and part of the characterization results concerning their microstructure, mechanical and tribological properties as well as the corrosion resistance of nanocomposite nc-WC/a-C and MoS₂(Ti,W) coatings deposited by magnetron sputtering onto Vanadis 23 HS steel and hardened Ti6Al4V titanium alloy substrates are presented and discussed. The work was accomplished by an interdisciplinary team of researchers from AGH University of Science and Technology in Krakow, the Motor Transport Institute in Warsaw and of the Lodz University of Technology in the frame of the POIG project KomCerMet (Workpackage KCM3) financed by the Ministry of Science and Higher Education of Poland.

Keywords: nanocomposites, coatings, nc-WC/a-C, MoS₂, nanostructure, dry friction, resistance to corrosion & wear, protection against galling

NANOKOMPOZYTOWE POWŁOKI SAMOSMARUJĄCE NA OSNOWIE Z AMORFICZNEGO WĘGLA BĄDŹ MoS₂ DLA PRZEMYSŁU MOTORYZACYJNEGO, LOTNICZEGO I KOSMICZNEGO

Większa wydajność i niezawodność, niższe zużycie paliwa i smarów, a także większa troska o środowisko naturalne - to dzisiaj główne siły napędowe postępu technicznego w motoryzacji, lotnictwie i przemyśle kosmicznym. Do skutecznych sposobów rozwiązywania tych problemów należą: obniżanie strat energii wskutek tarcia w układach przenoszenia napędu, jak również obniżenie wagi konstrukcji poprzez zastąpienie stalowych elementów mechanizmów i silników dwukrotnie lżejszymi, wykonanymi ze stopów tytanu. W pracy zawarto podstawowe informacje dotyczące wytwarzania dwóch rodzajów grubych nanokompozytowych powłok niskotarciowych na podstawie amorficznego węgla bądź MoS₂ osadzonych przez rozpylanie magnetronowe na podłożach ze stali Vanadis 23 i utwardzonego stopu tytanu Ti6Al4V oraz część wyników badań ich właściwości, w szczególności mikrostruktury, właściwości mechanicznych, tribologicznych oraz odporności na korozję, a także dyskusję tych wyników. Badania były wykonane w ramach projektu KomCerMet (pakiet KCM3) przez interdyscyplinarny zespół badawczy złożony z pracowników Akademii Górniczo-Hutniczej, Instytutu Transportu Samochodowego oraz Politechniki Łódzkiej w ramach Programu Operacyjnego POIG, finansowanego przez Ministerstwo Nauki i Szkolnictwa Wyższego.

Słowa kluczowe: nanokompozyty, powłoki, nc-WC/a-C, MoS₂, nano/mikrostruktura, tarcie suche, odporność na zużycie i korozję, ochrona przed zatarciem

INTRODUCTION

The application of modern advanced composites in the car or aviation industry or spacecraft construction decreases the weight and fuel consumption of vehicles and protects the environment against pollution [1, 2]. Simultaneously in the last decade, great effort has been

made to implement different surface treatments in the automotive or aviation industry in order to reduce friction and wear and increase the durability of numerous engine and powertrain parts [3-8]. A great part of these treatments consists in the deposition of different nano-

composite, self-lubricating coatings by means of different PVD or CVD techniques. The coatings were characterised by a low friction coefficient against metallic, ceramic and composite materials (~ 0.1), low intrinsic stress, good adhesion to numerous substrates and a characteristic composite structure consisting of nanocrystallites of, for instance, several transition metal carbides, embedded in an amorphous carbon or MoS₂ matrix. In addition, they were easy to deposit with the use of conventional CVD or PVD techniques (e.g. by magnetron sputtering). The first reports on these very useful properties of the coatings issued in the late 1990s by Dennis Teer Coatings Ltd. in Great Britain [9, 10] and by the US Air Force Laboratories [11]. That was the reason why in the frame of the POIG KomCerMet project (2008-2012), a series of different carbon-, MoS₂- and MoO₃-based self-lubricating coatings has been elaborated and characterized in an interdisciplinary team of researchers from AGH-UST in Krakow, MTI in Warsaw and LUT in Lodz. Part of the results are described in the present paper.

EXPERIMENTAL PROCEDURE

Thick (~ 1.5 and ~ 3 μm) nanocomposite coatings, nc-WC/a-C and MoS₂(Ti,W), respectively, were deposited onto 6 mm thick disk substrates 25.4 mm in diam. from Vanadis 23 High Speed steel and Ti6Al4V titanium alloy. The substrates were first hardened by quenching and tempering to 65HRC (in the case of Vanadis 23 steel) and to 1100 VHN0.05 by means of a diffusion hardening process with interstitial oxygen atoms according to a procedure described elsewhere [12] in the case of the titanium alloy substrate. After hardening, the specimens were mirror polished with use of a 3 μm grid diamond paste to a final roughness of 0.02 μm . The nanocomposite coatings were deposited by means of magnetron sputtering onto the face surface of the discs in a multipurpose vacuum stand B-90 equipped with 4 planar magnetrons described in [13]. In the case of the nc-WC/a-C coating deposition, three magnetrons were equipped with 4N pure graphite 9 mm thick targets and one magnetron with a 3N pure W target. In the case of the MoS₂(Ti,W) coatings deposition, two of the four magnetrons were equipped with sintered MoS₂ targets with 12 at.% Ti admixture, one with pure Ti grade 4 and one with 3N pure metallic tungsten. Before deposition, the vacuum chamber with the substrates was first evacuated to a residual pressure of 1×10^{-3} Pa and IR heated to approximately 500 K, next the surface of the specimens was cleaned in a glow discharge in 5N pure Ar plasma. In the next step, a thin intermediate layer of pure Ti was deposited (in the case of MoS₂(Ti,W) coating) or a gradient one starting from pure W with an increasing admixture of carbon atoms (in case of nc-WC/a-C coatings). In the final step, a thick nc-WC/a-C or MoS₂(Ti,W) coating was deposited. The parameters of chamber heating, glow dis-

charge cleaning, interlayer deposition or of the thick top nanocomposite nc-WC/a-C or MoS₂(Ti,W) coatings deposition were similar to (but not precisely the same) those given in two earlier papers [14] and [15]. After deposition, the specimens were left in the vacuum chamber at a residual pressure of 1×10^{-3} Pa to cool down to the ambient temperature.

The investigations of the coating nano/microstructures were carried out with scanning- and transmission electron microscopy (SEM, TEM). The SEM investigations were performed with use of a Zeiss NEON® 40EsB. The analytical TEM and HRTEM investigations were carried out with a JEOL JEM-2010 ARP (200 kV) and an FEI Titan³™ G2 60-300 (300 kV) microscope on the cross-section lamellae. The lamellas were prepared by a Zeiss Focused Ion Beam (FIB) NEON 40EsB CrossBeam followed by short ion-beam thinning using a Gatan Precision Ion Polishing System (PIPS). The phase identification was performed by means of selected area electron diffraction (SAED). The SAED and fast Fourier transformation (FFT) patterns were interpreted with the help of Java Electron Microscopy Software (JEMS) [16]. The phase identification was supplemented by energy dispersive X-ray spectroscopy microanalysis (EDX).

The hardness and indentation moduli of the coating/substrate systems were measured by means of nanoindentation experiments according to the ISO 14577-1 standard [17] using Vickers diamond and CSM Instruments equipment. The maximum load in the range 10–50 mN corresponds to 100–500 nm penetration depth. The indentation curves were analyzed according to the Oliver-Pharr procedure [18]. At a 10 mN load, the penetration depth was lower than 10% of the coating thickness, which excluded the effect of the substrate on the indentation results [19]. At least 6 indentations were performed for each sample, and for further analysis, the average value was taken into account. The adhesion of the coatings to the substrates, as well as their resistance to cracking was evaluated by the microscratch technique using a Rockwell C conical diamond stylus (angle at cone apex was 120°, radius of spherical tip was 200 μm) [20]. The scratch test was performed with an increasing load from 0 to 30 N, at a 5 mm/min speed and a scratch length of 5 mm. The average values calculated from the 3 scratches for each of the systems, as well as the failure modes are given in the text. Critical loads L_{C1} and L_{C2} corresponding to the cohesive and adhesive failures of the coatings were determined using acoustic emission intensity and post factum surface examination with optical microscopy. The tribological tests were performed according to the ISO 20808:2004 [21] standard on a ball-on-disc tribometer, using 6 mm diam. Al₂O₃ balls at a load (F_n) of 1 or 2.5 N. The maximum number of cycles (depending on the sample) was set to 20000. The tribological tests were repeated three times under the same testing conditions. The specific wear rate (W_V) was calculated from the wear volume of the disk material obtained from the

registered profiles of the wear track as: $W_V = V/(F_n \cdot L)$, where V is the volume of the removed material in mm^3 , F_n - load in Newtons and L - sliding distance in meters.

Electrochemical measurements were performed in a 0.5 M NaCl water solution. Voltametric measurements were carried out at a scan rate of 1 mV/s within the range of -100 to 1000 mV versus open circuit potentials and the polarization curves were recorded corresponding to every one of the examined samples. Prior to each polarization experiment, the samples were immersed in the electrolyte for 1 hour while monitoring the open circuit potential to establish steady state conditions. A three-electrode cell arrangement was applied using the Ag/AgCl electrode with a Luggin capillary as a reference electrode and a platinum wire as the auxiliary electrode (counter electrode). The measurements were carried out by means of the AUTOLAB PGSTAT Autolab EcoChemie System type 302N with relevant software for experiment control, data acquisition and their analysis.

RESULTS AND DISCUSSION

Micro- and nano-structure characterization

nc-WC/a-C coatings

The coating thicknesses on hardened steel and titanium alloy substrates were 1.3 and 1.8 μm , respectively. A typical SEM image of the coating on steel is shown in Figure 1.

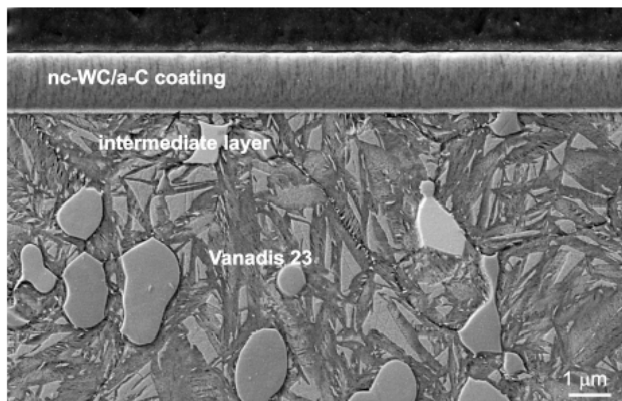


Fig. 1. Microstructure of nc-WC/a-C coating on Vanadis 23 steel. SEM image

Rys. 1. Mikrostruktura powłoki nc-WC/a-C na stali Vanadis 23. Obraz SEM

Both coatings have a columnar morphology (Fig. 2a), characteristic for zone "T" in Thornton's zone structure model [22]. The electron diffraction patterns taken from the coatings were diffused and difficult for unequivocal interpretation. It was found during the HRTEM investigation that the coating is composed of nanocrystallites (of a size $2\div 5$ nm) embedded in an amorphous carbon matrix (Fig. 2b). Analysis of the fast Fourier transformation (FFT) patterns and interplanar

spacing measurements for particular crystals showed a presence of different tungsten carbides, mainly $\text{WC}_{0.98}$ (face-centered cubic; fcc), W_2C (trigonal primitive; tp) and W_3C (cubic primitive; cp) in the coating.

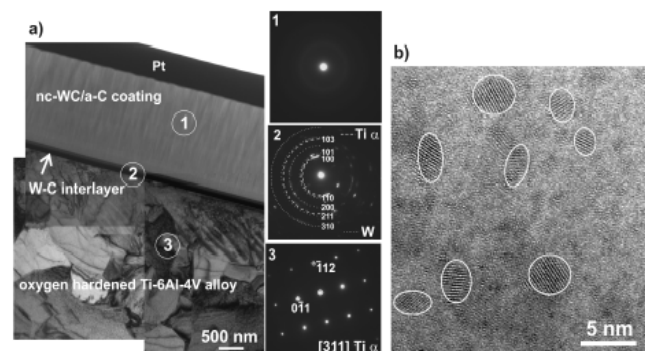


Fig. 2. a) Microstructure of nc-WC/a-C coating on oxygen hardened Ti-6Al-4V alloy as well as SAED patterns (1-3) taken from corresponding areas marked on TEM image and their identification. TEM, cross-section FIB lamella; b) HRTEM micrograph of coating

Rys. 2. a) Mikrostruktura powłoki nc-WC/a-C na utwardzonym stopie Ti6Al4V. Obraz TEM; b) Obraz HRTEM tej samej powłoki

A 50 and 160 nm thick W-C gradient interlayer was present between the nc-WC/a-C coating and the substrate material (steel and titanium alloy, respectively). Analyses of the SAED patterns confirmed that a W_α phase (body-centered cubic; bcc) is present in the interlayer. The STEM-EDS line analysis showed a gradient of concentration of W atoms in the interlayer, which decreased in the direction from the substrate (titanium alloy or steel) to the coating.

MoS₂(Ti,W) coatings

The coating thickness was 3.1 μm on both substrate materials (Fig. 3). An incomplete ring with interplanar spacing close to the $\{002\}$ planes of MoS_2 was clearly visible in the electron diffraction patterns taken from an FIB lamella. The results of micro-/nanostructural analyses performed by HRTEM showed that the coatings are composed of nanoclusters (of a size $3\text{ nm}\div 8\text{ nm}$) embedded in an amorphous matrix (Fig. 4a). The HRTEM images show numerous short black lines with a spacing of $0.615\div 0.68$ nm assigned to the MoS_2 clusters. The $\{002\}$ planes of nanoclusters were differently oriented to the surface of the coating, but in the near-to-surface zone of the coating they were in general parallel to the coating surface (Fig. 4b). Interplanar spacing measurements for particular crystals and FFT analyses also revealed a presence of some $\text{Ti}\alpha$ (hexagonal close-packed, hcp), W_α (body centered cubic, bcc) and Ti_2S (orthorhombic primitive, op) nanocrystallites of the size $4\div 8$ nm in the coating.

An intermediate layer ~ 20 nm thick, deposited in order to increase the coating adhesion to the substrate, was present between the coating and the substrate (Fig. 3). The SAED analysis revealed that this interlayer is composed of a Ti_α phase (hexagonal close-packed; hcp).

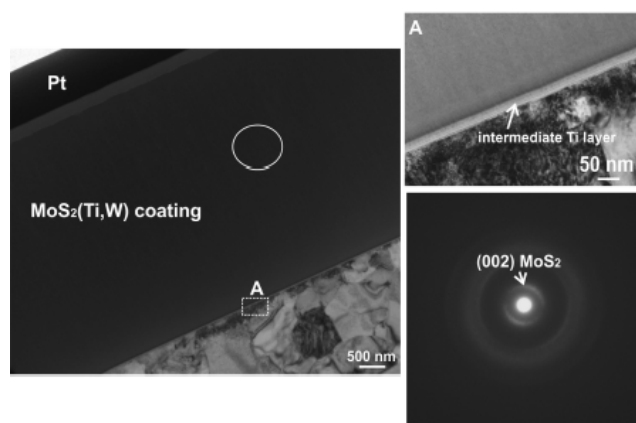


Fig. 3. Microstructure of MoS₂(Ti,W) coating on oxygen hardened Ti-6Al-4V alloy and magnified details of area close to interlayer as well as SAED pattern taken from coating area marked on figure as a circle. TEM image from FIB lamella

Rys. 3. Mikrostruktura powłoki MoS₂(Ti,W) na utwardzonym stopie Ti6Al4V i powiększone wybrane obszary tej powłoki. Obraz TEM

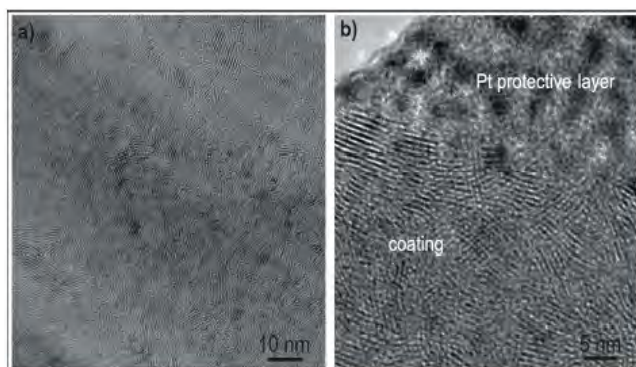


Fig. 4. HRTEM micrographs of MoS₂(Ti,W) coating on oxygen hardened Ti-6Al-4V alloy: a) coating micro structure overview; b) near-to-surface zone of structure overview

Rys. 4. Obraz HRTEM powłoki MoS₂(Ti,W) na utwardzonym podłożu Ti6Al4V: a) obraz ogólny; b) powiększony obraz obszaru w pobliżu powierzchni powłoki

Indentation and tribological characterization

The indentation tests showed that the hardness of the nc-WC/aC coatings is about 14 GPa. The hardness values of both samples with the coating decrease to that of the hardness at higher indentation loads [19]. The nc-WC/aC coating is also characterised by a low elastic modulus $E = 170\div 180$ GPa. Such a value is similar to that of numerous substrates like steels and hardened titanium alloys. The low mismatch between the stiffness of the coating and that of the substrate prevents high stress concentration at the coating-substrate interface and provides greater resistance to contact load [23]. Contrary to that, the MoS₂(Ti,W) coatings are significantly softer ($6.6\div 6.7$ GPa) and the corresponding elasticity modulus is also lower ($E = 100\div 108$ GPa). Brittle cracks at indent corners and sides were not found in any of tested coatings, even at maximum indentation load $F = 50$ mN. The results of the indentation tests are summarized in Table 1.

TABLE 1. Results of indentation tests
TABELA 1. Wyniki testów indentacyjnych

Coating-substrate system	Tribological tests		Scratch tests	
	$W_v \cdot 10^{-6}$ [mm ³ /Nm]	f	L_{C1} [N]	L_{C2} [N]
nc-WC/a-C on Ti6Al4V(O ₂)	0.08 ± 0.01	0.06	4.9	12.4
nc-WC/a-C on VANADIS 23	0.07 ± 0.01	0.05	6.2	13.0
MoS ₂ (Ti,W) on Ti6Al4V(O ₂)	0.26 ± 0.02	0.15 (initial) 0.1 (stable)	4.7	11
MoS ₂ (Ti,W) on VANADIS 23	0.25 ± 0.02	0.2 (initial) 0.07 (stable)	19	24

The tribological properties of the coatings (friction coefficient and wear resistance) were determined against an alumina ball (Fig. 5). During friction up to 20000 cycles at a load of 1N, distinct wear behaviour of the MoS₂(Ti,W) coatings was ascertained at a wear rate equal to $0.25 \cdot 10^{-6}$ mm³/J for the coating on Vanadis 23 and $0.26 \cdot 10^{-6}$ mm³/J on the oxygen hardened Ti6Al4V substrate. In contrast to that, the wear rates of the nc-WC/a-C coatings were much lower. That was the reason why during the tribological tests of these coatings a higher load of 2.5 N was applied. The nc-WC/a-C coatings, irrespective of the substrate, exhibited similar resistance to wear, namely $0.07 \cdot 10^{-6}$ mm³/Nm for the coating on Vanadis 23 and $0.08 \cdot 10^{-6}$ mm³/Nm for the coating on the titanium alloy. In none of the tribological tests was the coating totally abraded from the substrate. The results of the tribological and scratch tests are summarized in Table 2.

TABLE 2. Scratch and tribological tests results
TABELA 2. Wyniki testów tribologicznych oraz zarysowania

Coating-substrate system	F [mN]	h_{max} [nm]	H_{IT} [GPa]	E_{IT} [GPa]
nc-WC/a-C on Ti6Al4V(O ₂)	10	168±9	14.3±0.9	176±12
	20	260±4	12.7±0.6	174±2
	50	456±12	12.6±0.9	165±11
nc-WC/a-C on VANADIS 23	10	172±2	13.6±0.4	170±9
	20	261±6	13.9±0.7	174±10
	50	427±8	13.9±0.2	192±18
MoS ₂ (Ti,W) on VANADIS 23	10	242±15	6.6±0.9	108±13
	20	348±9	6.9±0.5	121±8
	50	552±20	7.6±0.6	138±7
MoS ₂ (Ti,W) on Ti6Al4V(O ₂)	10	235±10	6.7±0.6	100±6
	20	326±8	7.5±0.3	116±8
	50	579±13	6.8±0.5	107±9

More than three times greater wear resistance of the nc-WC/a-C coatings in comparison to that for the MoS₂(Ti,W) ones was due to the greater load carrying capacity of the former in agreement with their twice greater hardness (Tab. 1). Therefore, the friction coefficient of the nc-WC/a-C coatings was lower as well. The wear of these coatings exhibited an abrasive nature and

proceeded almost uniformly except for a short initial period when the abrasion of the coatings was more intense. There were no deep scratches in the wear track or big buckling on either side of the groove.

The friction process proceeded stably in several stages: in the initial period - when the contact was being formed - the resistance to motion was larger, in the second step it decreased until a tribolayer was formed [14] which ensured stable cooperation and a very low friction coefficient below 0.1 (Fig. 5).

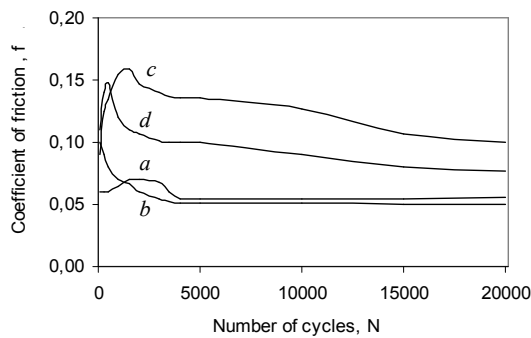


Fig. 5. Friction coefficient of nc-WC/a-C coating on Ti6Al4V alloy (a) and VANADIS 23 steel (b) as well as of the MoS₂(Ti,W) coating on Ti6Al4V alloy (c) and Vanadis 23 steel (d) against alumina ball

Rys. 5. Współczynnik tarcia powłoki nc-WC/a-C na stopie Ti6Al4V (a) i stali VANADIS 23 (b) oraz powłoki MoS₂(Ti,W) na stopie Ti6Al4V (c) i stali VANADIS 23 (d) podczas tarcia względem kulki Al₂O₃

Coating adhesion

For the nc-WC/a-C coatings, irrespective of the substrate, formation of the first cohesive cracks was observed at 5÷6 N. An increase in the load to 12÷13 N provoked coating delamination and exposure of large areas of substrate inside and outside of the scratch tracks. A similar character of failure during scratching revealed the softer MoS₂(Ti,W) coating on the titanium alloy substrate. On the other hand, the MoS₂(Ti,W) coating has better adhesion to the Vanadis 23 steel substrate. The first cohesive cracks appeared only when the load upon the indenter increased to 19 N (Fig. 6a). At a load of 24 N, adhesive cracks formed as small chips (Fig. 6b). It should be noted that the failure of this coating was not as catastrophic as that of the other one.

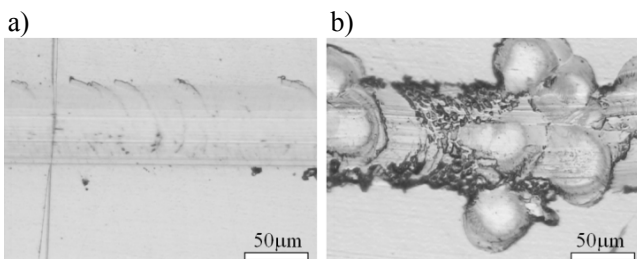


Fig. 6. Scratch track images of MoS₂(Ti,W) coatings on Vanadis 23 substrate under: a) $L_{c1} = 19$ N; b) $L_{c2} = 24$ N. LM, magn. x 200

Rys. 6. Obrazy toru zarysowania powłoki MoS₂(Ti,W) na stali Vanadis 23 przy obciążeniu: a) $L_{c1} = 19$ N; b) $L_{c2} = 24$ N. Mikroskop świetlny. Pow. x200

Resistance to corrosion

The corrosion current densities (i_{corr}) and corrosion potentials (E_{corr}) were obtained from the polarization curves by extrapolation of the cathodic and anodic branches of the polarization curves to the corrosion potential [24]. The results of the electrochemical measurements are given in Table 3. In the case of Vanadis 23 HS steel (Fig. 7), the smallest corrosion current density (and therefore the best resistance to corrosion) was obtained for the sample with the nc-WC/a-C coating, however, the difference between the corrosion current for the coated sample and the as-received one is very small. For the sample with the self-lubricating MoS₂(Ti,W) coating, the i_{corr} value was the biggest and this material had the lowest resistance to corrosion. On the other hand, the corrosion potential E_{corr} for the same sample was greater than that of the as-received and nc-WC/a-C coated ones.

TABLE 3. Electrochemical corrosion parameters of samples obtained from polarization curves

TABELA 3. Parametry korozyjne wyznaczone na podstawie wykresów polaryzacyjnych

Coating	Substrate			
	Vanadis 23HS steel		Ti6Al4V	
	E_{corr} [mV _{Ag/AgCl}]	i_{corr} [μA/cm ²]	E_{corr} [mV _{Ag/AgCl}]	i_{corr} [μA/cm ²]
---	-594	2.6	-9	0.01
nc-WC/a-C	-447	2.2	30	0.02
MoS ₂ (Ti, W)	-393	15.7	29	0.03

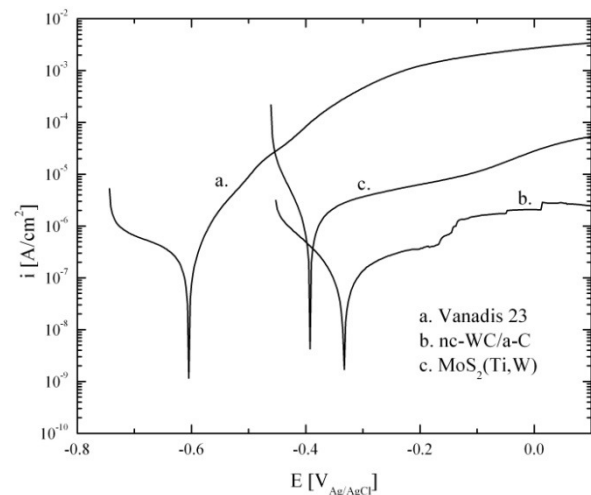


Fig. 7. Polarization curves of Vanadis 23 HS steel in 0.5 M NaCl

Rys. 7. Krzywe polaryzacji w 0.5 M roztworze NaCl dla podłoża Vanadis 23 bez powłok i z powłokami

For the titanium alloy substrate in the 0.5 M NaCl solution, the corrosion current densities for all the samples (one as received and two coated ones) were very low, however, the lowest value was obtained for the as-received Ti6Al4V alloy (Fig. 8 and Tab. 3). In the 0.5 M water solution of NaCl, the values of the corrosion potentials for the coated titanium alloy sub-

strate were greater than .0 V and almost equal to each other (.029 V and .030 V) in contrast to the as-received Ti6Al4V alloy for which the potential was slightly less than .0 V (-9 mV). Nevertheless, no pitting corrosion was observed on any of the tested samples with the Ti6Al4V substrate.

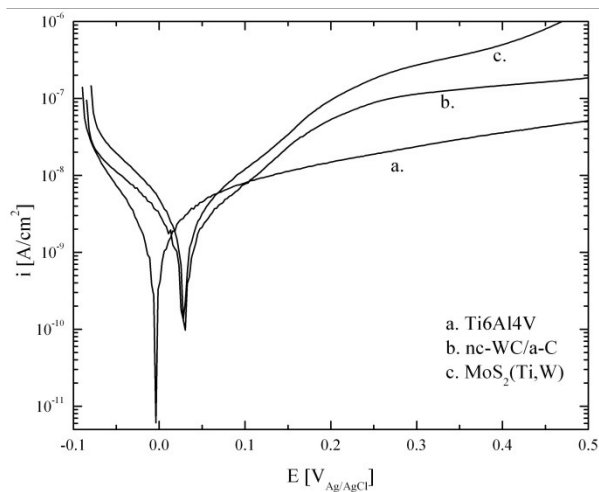


Fig. 8. Polarization curves of hardened Ti6Al4V alloy in 0.5 M NaCl

Rys. 8. Krzywe polaryzacji w 0.5 M roztworze NaCl dla utwardzonego podłoża ze stopu Ti6Al4V bez powłok i z powłokami

SUMMARY

The tribological tests carried out in dry friction conditions give evidence of very good sliding properties of both types of the investigated coatings (coefficient of friction below 0.1). As concerns the wear resistance, in the case of the nc-WC/a-C coating, irrespective of the substrate, it was three times greater than that for MoS₂(Ti,W). This is plausibly due to the more than twice greater hardness of the former. It is worth mentioning that the remarkable resistance to wear of the nanocomposite nc-WC/a-C coating equal to $8 \cdot 10^{-17} \text{ m}^3/\text{N} \cdot \text{m}$ corresponds to a very high energy wear coefficient equal to $\sim 5 \text{ GJ/g}$, which means that 5 GJ of energy is necessary for abrading 1 g of the nc-WC/a-C coating during dry friction in the conditions of the performed tribotests. It is well evident that such coatings can protect well the contacting surfaces of moving parts from titanium alloys or steels against galling or seizing.

The resistance to corrosion of the as-received titanium alloy Ti6Al4V and the one with either of the investigated nanocomposite selflubricating coatings estimated from the polarization curves were rather similar (i_{corr} values of corrosion currents of all samples with Ti6Al4V substrate in 0.5 M water solution of NaCl are of the order of $1 \cdot 10^{-8} \text{ A} \cdot \text{cm}^2$). In comparison to this result, the resistance to corrosion of the samples (coated and as-received ones) with the substrate from Vanadis 23 steel is much worse. Nevertheless, once again the resistance to corrosion of the samples with the nc-WC/a-C coating was the greatest from all the investigated samples with the steel substrate.

The obtained results give evidence that titanium alloys are useful engineering materials due to the useful combination of their high strength-to-weight ratio and corrosion stability in a wide range of environments. Pure titanium and titanium alloys are highly corrosion resistant in aqueous solutions even with aggressive chloride anionic species. The nanocomposite, self-lubricating coatings deposited by the magnetron sputtering method have not changed the very good resistance to corrosion of the titanium alloy: no pitting corrosion was observed on any of the tested samples with the Ti6Al4V substrate. On the other hand - these nanocomposite coatings on hardened titanium alloy substrates increase their resistance to wear by several orders of magnitude.

Acknowledgements

The results presented in this paper were obtained within the "KomCerMet" project (contract no. POIG.01.03.01-14-013/08-00 with the Polish Ministry of Science and Higher Education) in the framework of the Innovative Economy Operational Programme 2007-2013.

REFERENCES

- [1] Idzior M., Changes in materials technologies for automotive industry provoked by ecology, *Metrol.* 2007, 9, 72-87 (in Polish).
- [2] Williams J.C., Starke E.A., Jr., Progress in structural materials for aerospace systems. *Acta Materialia* 2003, 51, 5775-5799.
- [3] Mitterer C., Lechtaler M., Gassner G., Fontalvo G.A., Toth L. et al, Selflubricating chromium carbide/amorphous hydrogenated carbon nanocomposite coatings: a new alternative to tungsten carbide/amorphous hydrogenated carbon, *Proc. of the Institution of Mechanical Engineers* 223 (J5), suppl. Special Issue on Tribology Research in Austria, Aug. 2009, 751-757.
- [4] Vetter J., Crummenauer J., Barbezat G., Avissar J., Surface treatments of automotive parts - research and applications, *Vakuum in Forschung und Praxis* 2008, 20, 1, 28 May, 47-52.
- [5] Vetter J., Barbezat G., Surface enhancements for automotive applications low friction, hard and corrosion resistant, *Sulzer Technical Review* 2007, 1, 8-11.
- [6] Vetter J., Crummenauer J., Barbezat G., Avissar J., Surface treatment selections for automotive applications, *Surface & Coatings Technology* 2005, 200, 1962-1968.
- [7] Gahlin R., Larsson M., Hedenquist P., ME-C:H coatings in motor vehicles, *Wear* 2001, 249, 302-309.
- [8] Gili F., Mangherini D., Igartua A., Fernandez X., Wendler B., Laboratory screening of novel coating grades applied to key powertrain components, Plenary lecture during the 3rd AIT Workshop of the Italian Association of Engineers in Milano, Italy, 22-23 February 2012.
- [9] Teer D.G., Hampshire J.H., GB Patent 2,258,343 March 1991.
- [10] Teer D.G., Bellido V., GB Patent 2,303,380 (1996).
- [11] Voevodin A.A., O'Neill J.P., Zabinski J.S., Nanocomposite tribological coatings for aerospace applications, *Surface and Coatings Technology* 1999, 116-119, 36-45.

- [12] Wendler B.G., Liskiewicz T., Kaczmarek L., Januszewicz B., Rylska D., Fouvry S., Rylski A., Jachowicz M., in: G. Luetjering, J. Albrecht (Eds.), Oxygen diffusion strengthening of Ti6Al4V alloy in glow discharge plasma. *Ti-Science and Technology*, Vol. 2, Wiley-VCH, Weinheim 2004, 905-912.
- [13] Wendler B., Danielewski M., Przybylski K., Rylski A., Kaczmarek L., Jachowicz M., New type AlMo-, AlTi- or Si-based magnetron sputtered protective coatings on metallic substrates, *Journal of Materials Processing Technology* 2006, 175, 427-432.
- [14] Moskalewicz T., Wendler B., Zimowski S., Dubiel B., Czyrska-Filemonowicz A., Microstructure, micro-mechanical and tribological properties of the nc-WC/a-C nanocomposite coatings magnetron sputtered on non-hardened and oxygen hardened Ti-6Al-4V alloy. *Surface and Coatings Technology* 2010, 205, 2668-2677.
- [15] Pawlak W., Wendler B., Nolbrzak P., Makówka M., Włodarczyk K., Rylski A., Low friction MoS₂(Ti,W) coatings deposited by magnetron sputtering, *Inżynieria Materiałowa* 2010, 3, 418-421.
- [16] Stadelmann P., JEMS Java Electron Microscopy Software, 2004, <http://cime.epfl.ch>.
- [17] Thornton J.A., *Journal of Vacuum Science and Technology* 1986, A 4, 3059-3065.
- [18] ISO 14577-1. Metallic materials - instrumented indentation test for hardness and material parameters - part 1: test method.
- [19] Oliver W.C., Pharr G.M., An improved technique for determining hardness and elastic modulus using load and displacement sensing indentation experiments, *Journal of Materials Resources* 1992, 7, 1564-83.
- [20] Kot M., Lacki P., Contact mechanics of coating-substrate systems: I - Methods of analysis and FEM modeling of nanoindentation tests, *Journal of the Balkan Tribological Association* 2012, 18, 598-614.
- [21] Kot M., Moskalewicz T., Wendler B., Czyrska-Filemonowicz A., Rakowski W., Micromechanical and tribological properties of nanocomposite nc-TiC/a-C coatings, *Solid State Phenomena* 2011, 177, 36-46.
- [22] ISO 20808:2004. Fine ceramics (advanced ceramics, advanced technical ceramics) - determination of friction and wear characteristics of monolithic ceramics by ball-on-disc method.
- [23] Kot M., Major Ł., Lackner J., Rakowski W., Analysis of spherical indentations of coating-substrate systems: experiments and finite element modeling, *Materials and Design* 2013, 43, 99-111.
- [24] Wang J., *Analytical Electrochemistry*, 2nd Edition, Wiley-VCH, Hoboken 2000.